



Research Article

Cardiotoxicity Evaluation of Tyrosine Kinase Inhibition using Human Induced Pluripotent Stem Cell-derived Healthy and Long QT Syndrome Cardiomyocytes

Qi Zhao^{1,2#}, Yizhe Zhang^{2#}, Yuqing Zhang^{1,2}, Yiyang Teng¹, Shuwen Yang^{1,2}, Hao Yang¹, Hongyan Xing², Xijie Wang^{1,2*}

Abstract

Tyrosine kinase inhibitors (TKIs) are small-molecule targeted therapy drugs that play an important role in the treatment of hematological malignancies and solid tumors. Drug-induced cardiotoxicity in both preclinical studies and clinical trials has been reported, whereas the toxicity in populations with congenital electrophysiological dysfunction remains unclarified. Hence, an investigation of TKIs toxicological research helps assess the drug response in patients, predicting cardiotoxicity risk, and providing a reference for clinical application. We investigate the cardiotoxicity of four tyrosine kinase inhibitors (Crizotinib, Sunitinib, Dasatinib, and Lapatinib) with different targets using cardiomyocytes differentiated from disease-specific human-induced pluripotent stem cells derived from WT- and Long QT syndrome patient (WT- and LQT-hiPSC-CMs) combined with real-time cell analysis (RTCA), immunofluorescence, and chemiluminescence. In this study, Crizotinib, Sunitinib, and Lapatinib caused cardiotoxicity by reducing contractility, damaging the cell structure, and activating the Caspase-3/7 pathway supply. Dasatinib showed a lower risk of cardiotoxicity compared with the other three candidates. Compared with WT-hiPSC-CMs, LQT-hiPSC-CMs showed a higher sensitivity to Crizotinib and Sunitinib-induced cardiotoxicity. Our study indicates that congenital channelopathies, such as LQTS, may predispose patients to even higher risks, which require particular monitoring for the occurrence of adverse cardiac events.

Keywords: HiPSC-CMs; LQT; Cardiotoxicity; RTCA cardio system; Tyrosine kinase; Immunofluorescence; Caspase-3/7 pathway.

Introduction

The clinical application of molecular-targeted tyrosine kinase inhibitors (TKIs) has revolutionized the treatments of cancer; however, cardiovascular toxicities are frequent critical issues in patients [1]. Manifestations of cardiotoxicities of TKIs vary, including cardiac dysfunction, arrhythmias, and vascular and pericardial diseases. Current research suggests that TKIs target receptors and cytoplasmic kinases [2]. Therefore, preclinical prediction of cardiotoxicity is important in the evaluation of novel TKIs. To date, human-induced pluripotent stem cell-derived cardiac myocytes (hiPSC-CMs) provide an ideal platform for drug development. Compared with animal models, hiPSC-CMs have no species and extrapolation limitations. In addition, in contrast to non-cardiac human cell lines, hiPSC-CMs express the native cardiac proteins required to reconstitute the complex cardiac structure and phenotype (e.g., sarcomere organization, calcium

Affiliation:

¹China State Institutes of Pharmaceutical Industry, Shanghai, China

²Shanghai Innostar Bio-Tech Co, Ltd

*Corresponding author:

Xijie Wang, China State Institutes of Pharmaceutical Industry, Shanghai, China and Shanghai Innostar Bio-Tech Co, Ltd.

Citation: Qi Zhao, Yizhe Zhang, Yuqing Zhang, Yiyang Teng, Shuwen Yang, Hao Yang, Hongyan Xing, Xijie Wang. Cardiotoxicity Evaluation of Tyrosine Kinase Inhibition using Human Induced Pluripotent Stem Cell-derived Healthy and Long QT Syndrome Cardiomyocytes. *Archives of Clinical and Biomedical Research*. 8 (2024): 54-72.

Received: January 29, 2024

Accepted: February 05, 2024

Published: March 07, 2024

handling, metabolism, and electrophysiology) [3]. Moreover, patient-specific hiPSC-CMs provide an avenue to study the precise mechanism of the effects of human genetic mutations on cellular phenotypes. Different patient responses to specific drugs are jointly driven by interactions between genetic, epigenetic, and environmental factors, genetic polymorphisms of drug-metabolizing enzymes, transporters, target enzymes, ion channels, and receptors can affect pharmacodynamics [4]. Genotype-specific cardiotoxicity phenotypes can be mimicked in patients exposed to drugs by using patient-specific hiPSC-CMs, and can also observe compensatory mechanisms that are difficult to observe in animal models, based on which researchers can accurately analyze disease phenotypes and drug responses [5]. The earliest report of disease modeling based on hiPSC-CMs was derived from hiPSC-CMs from patients with Long QT syndrome (LQTS). Inherited forms of LQTS are caused by mutations in genes encoding cardiac ion channels. More than 20 pathogenic genes for LQTS have been identified, among which *KCNQ1* (LQT1), *KCNH2* (LQT2), and *SCN5A* (LQT3) are the most common pathogenic genes, hiPSC-CMs from *KCNQ1*-mutated patients exhibited a marked prolongation of action potential duration and a decrease in IKs current [6]. Therefore, two cell models of WT- and LQT-specific hiPSC-CMs were used in this experiment to evaluate TKI-induced cardiotoxicity, predict the risk of cardiotoxicity, and provide a reference for its clinical medication.

Firstly, we use WT- and LQT-hiPSC-CMs for the prediction of cardiotoxicity of TKIs by examination with the xCELLigence Real-Time Cell Analysis (RTCA) Cardio System, RTCA has been previously reported as an emerging method to quantify cardiac [7], and it can monitor the growth curve and beating state of cardiomyocytes differentiated from human induced pluripotent stem cells. Secondly, the effects of TKIs on myocardial structure and Cardiac Troponin T (cTnT) expression were evaluated on WT- and LQT-hiPSC-CMs. Finally, the effects of TKI on the activation of apoptotic pathways in WT- and LQT-hiPSC-CMs were investigated. The current study may shed light on the evaluation of cardiac toxicity effects of TKIs.

Materials and Method

Cell culture

WT-hiPSC-CMs and LQT-hiPSC-CMs were purchased from Cellapy (CA2101106, Beijing, China) and HELP (HELP4120, Nanjing, China), respectively. Both cell types were obtained as frozen 1 mL aliquots containing approximately 1 and 2 million cells, respectively. The cells were thawed and plated in 96-well E-plates (ACEA Biosciences, Hangzhou, China) pre-coated with 0.1% gelatin. The cells were incubated in a maintenance medium at 37 °C in an atmosphere of 5% CO₂, and the culture medium was

refreshed every 2 days. The WT and LQT cells were plated at densities of 3×10⁴ and 6×10⁴ cells/well, respectively. After beating stably, these two cells were used to study the electrophysiological characteristics and the activation pathway of apoptosis.

Real-time impedance-based bioanalyses of hiPSC-derived CMs

Spontaneous CM contraction and cell health were monitored in real-time by impedance using the xCELLigence® RTCA cardio system (ACEA Biosciences, Hangzhou, China). Impedance signals were monitored and recorded for 20 seconds per sweep as shown in Table 1. The cell index (CI), which is related to cell adherence and growth, was used as a measure of cell vitality.

Connexin 43 (CX-43) immunostaining on hiPSC-derived CMs

After drug treatment for 24 h, CX-43 immunostaining was performed. Cells were fixed using 4% PFA for 20 min at room temperature. Samples were then washed 3 times using a solution of PBS. The permeating sealer was added for 1 h at room temperature. Primary antibody CX-43-specific monoclonal antibodies (Invitrogen, C6219) were diluted at 1:100 in PBS and incubated for 12-20 h at 4 °C. Cells were then washed and the cell pellet was resuspended with the secondary antibody goat anti-mouse IgG (H+L) antibody (Invitrogen, A-11001) diluted 1:500 in PBS and incubated for 1 h in the dark. Cells were washed 3 times and 1 µg/mL Hoechst 33258 (Sigma-Aldrich, B1155) was added for 20 min in the dark. Finally, cells were washed 3 times and photographed immediately under a confocal laser microscope (LSM710, Zeiss, Germany).

Table 1: Data signal acquisition settings

Step	Sweep duration (second)	Sweeps	Interval (minute)	Comments
1	0	1	1	Baseline measurements
2	20	100	60	Monitoring
3	20	100	60	Monitoring
4	20	5	1	Before administration
5	20	12	5	After administration 1 h
6	20	4	15	After administration 2 h
7	20	8	30	After administration 3-6 h
8	20	100	60	After administration 7-24 h

Apoptosis Pathway Activation of hiPSC-derived CMs

Apoptosis was determined at 24 h post-drug treatment using Caspase-Glo 3/7 assay (Promega, Madison, WI, USA). Subsequently, the luminescence of cells was measured by the SpectraMax i3 multi-mode microplate reader (Molecular Devices, San Jose, CA, USA). At least three replicates of the cell apoptosis assay were conducted. At least two wells per drug dose were detected in each biological replicate.

Reagents

Four TKIs were investigated: Crizotinib, Dasatinib, Lapatinib (all from Sigma-Aldrich, St. Louis, MO, USA; PZ0191, CDS023389, and CDS022971, respectively), and Sunitinib (Aladdin, Shanghai, China; S126061). The TKIs and Thioridazine (Sigma-Aldrich, St. Louis, MO, USA; 1662504-200MG) were dissolved in dimethyl sulfoxide (Sigma-Aldrich, D4540) and the diluted drugs were equilibrated in a 37 °C, 5% CO₂ incubator for 30 min before being applied to the cells.

Data analysis and statistics

For RTCA CM monitoring, the CI, beating rate, beating amplitude, and half-maximal inhibitory concentration (IC₅₀) for each well were calculated offline using RTCA cardio software 1.0 and normalized to the corresponding baseline values measured before treatment with the compounds. A threshold level of 12 was used to suppress noise for improved peak recognition and the raw data of the beat curves were displayed using a threshold level of 0.

For Caspase-3/7 data analysis, the Caspase-3/7 detection result is expressed as the ratio of each concentration group and solvent control group, and the calculation formula is as follows: Caspase-3/7.

$$\text{content} = \frac{\text{drug luminescence value} - \text{vehicle control luminescence value}}{\text{solvent control group luminescence value} - \text{vehicle control luminescence value}}$$

The data are presented as means ± standard error of the mean (SEM) and the statistical significance of differences was estimated using a one-way analysis of variance (ANOVA) or Student's t-test. A value of $p \leq 0.05$ was considered significant.

Results

Analysis of the hiPSC-CMs based on marker protein expression and electrophysiological measurements revealed that the expected phenotypes were replicated in these cell models, namely that the WT-hiPSC-CMs had a normal phenotype and the LQT-hiPSC-CMs showed QT-interval prolongation. The relevant certificate of analysis is provided in the Supplementary data. Spontaneously contracting CMs were observed in both WT- and LQT-hiPSC-CMs as assessed by light microscopy.

The CI values increased and gradually stabilized with

the growth and adherence of both WT- and LQT-hiPSC-CMs (Figure S1A and S1C). Within 168 h after plating, the WT-hiPSC-CMs achieved a stable state in both beating rate and amplitude earlier than the LQT-hiPSC-CMs did (Figure S1B and S1D). The spontaneous beating rate of both WT- and LQT-hiPSC-CMs was stable at approximately 40 bpm, and the amplitude steadily increased over time and stabilized at approximately 0.09, with arrhythmic irregularity < 40% (Figure S2).

When both types of cell colonies were examined by fluorescence microscopy, an obvious decrease in CX-43 expression was noted in 20 μmol/L Thioridazine-treated cell colonies when compared with untreated cells. The CX-43 appeared as puncta located in or around some cell nuclear rather than between cell gaps in both types of cell colonies (Figure S3).

The effects of TKIs on WT-and LQT-hiPSC-CMs

Effects of Crizotinib: Crizotinib reduced the CI of both WT- and LQT-hiPSC-CMs in a concentration-dependent manner, indicating its inhibitory effect on the growth and adherence of cells at concentrations ≥ 3 μmol/L (Figure 1A and 1B). Crizotinib affected pulse signals of both WT- and LQT-hiPSC-CMs in a concentration-dependent manner and abolished the cellular automaticity at 3 μmol/L and 10 μmol/L, but the latter CMs showed signs of recovery at 3 μmol/L (Figure 1C and 1D). The beating rate reduced at concentrations ≥ 0.1 μmol/L in a concentration-dependent manner on WT- and LQT-hiPSC-CMs (Figure 1E and 1F). Analysis of the concentration-related effects of Crizotinib on WT- and LQT-hiPSC-CMs demonstrated IC₅₀ values of 0.89 μmol/L and 0.76 μmol/L, respectively (Table 2).

When both types of cell colonies were examined by fluorescence microscopy, increased CX-43 expression around some cell nuclear and decreased CX-43 expression between cell gaps were noted at ≥ 1 μmol/L on Crizotinib-treated WT- and LQT-hiPSC-CMs colonies and the CX-43 expression between the gaps of LQT-hiPSC-CMs was less than that of WT-hiPSC-CMs at the same concentration. (Figure 2A and 2B). Crizotinib could increase the activity of Caspase-3/7 protein in a concentration-dependent manner at ≥ 3 μmol/L on WT-hiPSC-CMs and at ≥ 1 μmol/L on LQT-hiPSC-CMs (Figure 2C).

Table 2: Comparison of WT-hiPSC-CMs with LQT-hiPSC-CMs

TKI	IC ₅₀ (μmol/L)	
	WT-hiPSC-CMs	LQT-hiPSC-CMs
Crizotinib	0.89	0.76
Sunitinib	4.71	0.52
Dasatinib	27.34	23.3
Lapatinib	6.87	10.89

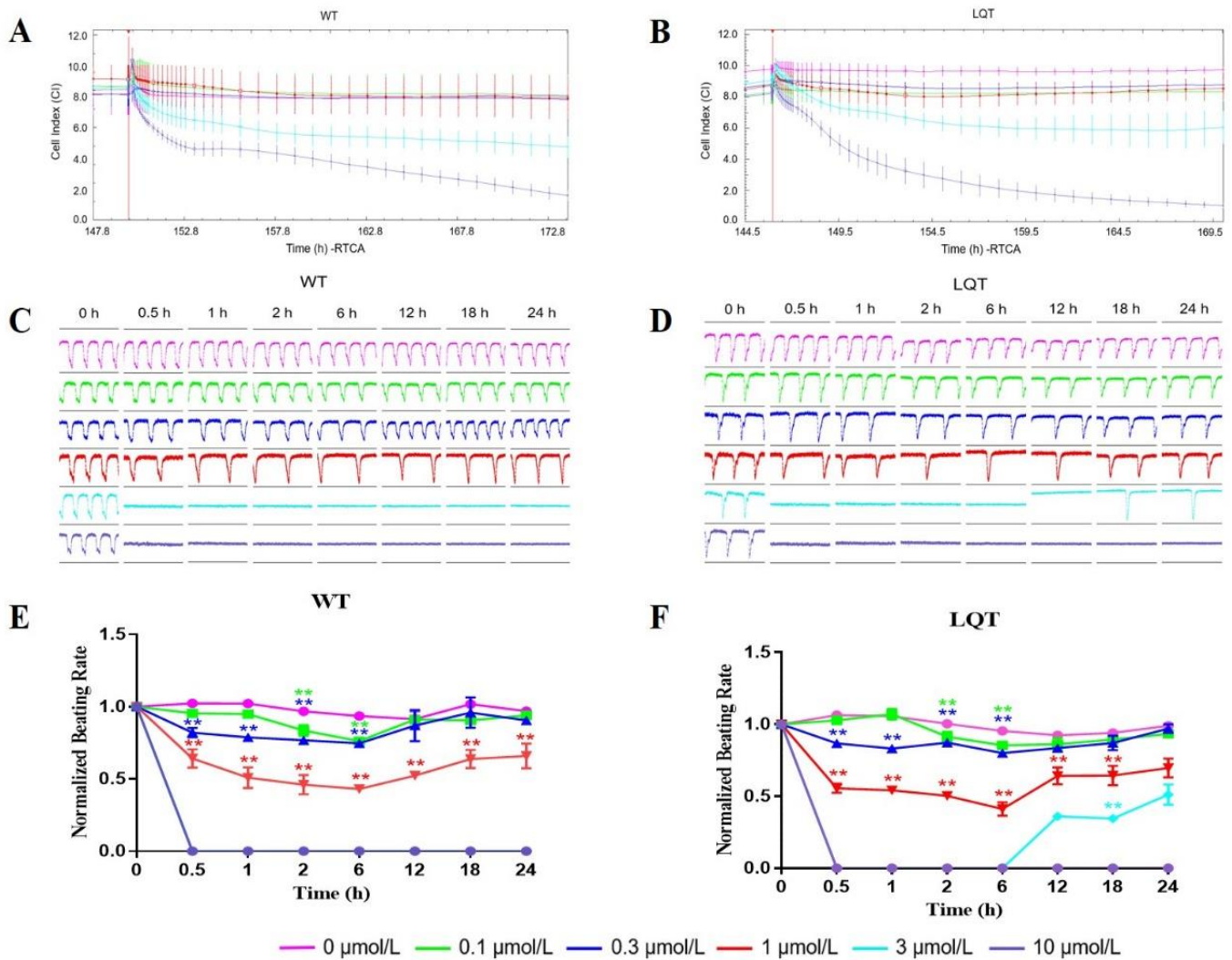


Figure 1: Effects of Crizotinib on WT- and LQT-hiPSC-CMs. Effect of Crizotinib on cell index (CI) of A WT- and B LQT-hiPSC-CMs. Effect of Crizotinib on transient pulse patterns of C WT- and D LQT-hiPSC-CMs. Effect of Crizotinib on beating rate of E WT- and F LQT-hiPSC-CMs. Data are means \pm standard error of the mean (SEM) of $n = 3-6$ experiments. * $p < 0.05$ and ** $p < 0.01$ compared to control (DMSO).

Effects of Sunitinib: Sunitinib reduced the CI of both WT- and LQT-hiPSC-CMs at 10 $\mu\text{mol/L}$ (Figure 3A and 3B). Sunitinib affected pulse signals of both WT- and LQT-hiPSC-CMs in a concentration-dependent manner and abolished the cellular automaticity at 10 $\mu\text{mol/L}$ for WT-hiPSC-CMs while at 1 $\mu\text{mol/L}$ for LQT-hiPSC-CMs. (Figure 3C and 3D). The beating rate reduced at concentrations $\geq 0.3 \mu\text{mol/L}$ in a concentration-dependent manner on WT- and LQT-hiPSC-CMs (Figure 3E and 3F). Evaluation of the concentration-dependent effects of Sunitinib on WT- and LQT-hiPSC-CMs demonstrated IC_{50} values of 4.71 $\mu\text{mol/L}$ and 0.52 $\mu\text{mol/L}$, respectively (Table 2).

When both types of cell colonies were examined by fluorescence microscopy, increased CX-43 expression around some cell nuclear and decreased CX-43 expression

between cell gaps were noted at $\geq 1 \mu\text{mol/L}$ on Sunitinib-treated WT- and LQT-hiPSC-CMs colonies and the CX-43 expression between the gaps of LQT-hiPSC-CMs was less than that of WT-hiPSC-CMs at the same concentration. (Figure 4A and 4B). Sunitinib could increase the activity of Caspase-3/7 protein in a concentration-dependent manner at $\geq 3 \mu\text{mol/L}$ on WT-hiPSC-CMs and at $\geq 0.1 \mu\text{mol/L}$ on LQT-hiPSC-CMs (Figure 4C).

Effects of Dasatinib: Dasatinib does not affect the CI values of both WT- and LQT-hiPSC-CMs (Figure 5A and 5B). Dasatinib affected pulse signals of both WT- and LQT-hiPSC-CMs in a concentration-dependent manner and abolished the cellular automaticity at 30 $\mu\text{mol/L}$ on LQT-hiPSC-CMs (Figure 5C and 5D). The beating rate of WT-hiPSC-CMs reduced in a concentration-dependent

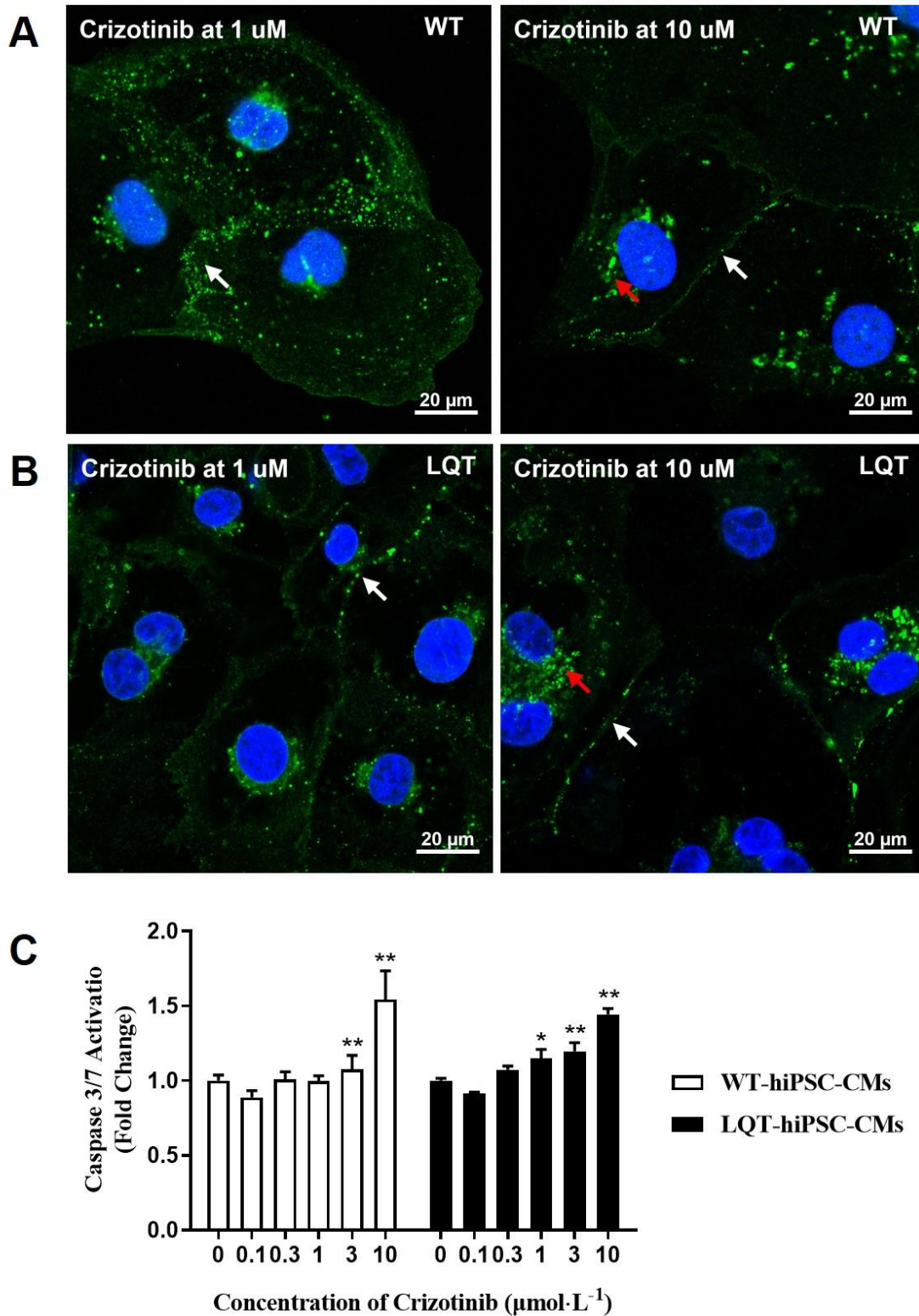


Figure 2: Effect of Crizotinib on CX-43 expression of A WT- and B LQT-hiPSC-CMs. C Effect of Crizotinib on Caspase-3/7 activation in WT- and LQT-hiPSC-CMs. Data are means \pm standard error of the mean (SEM), $n = 3$. * $p \leq 0.05$ and ** $p \leq 0.01$ compared to control (DMSO).

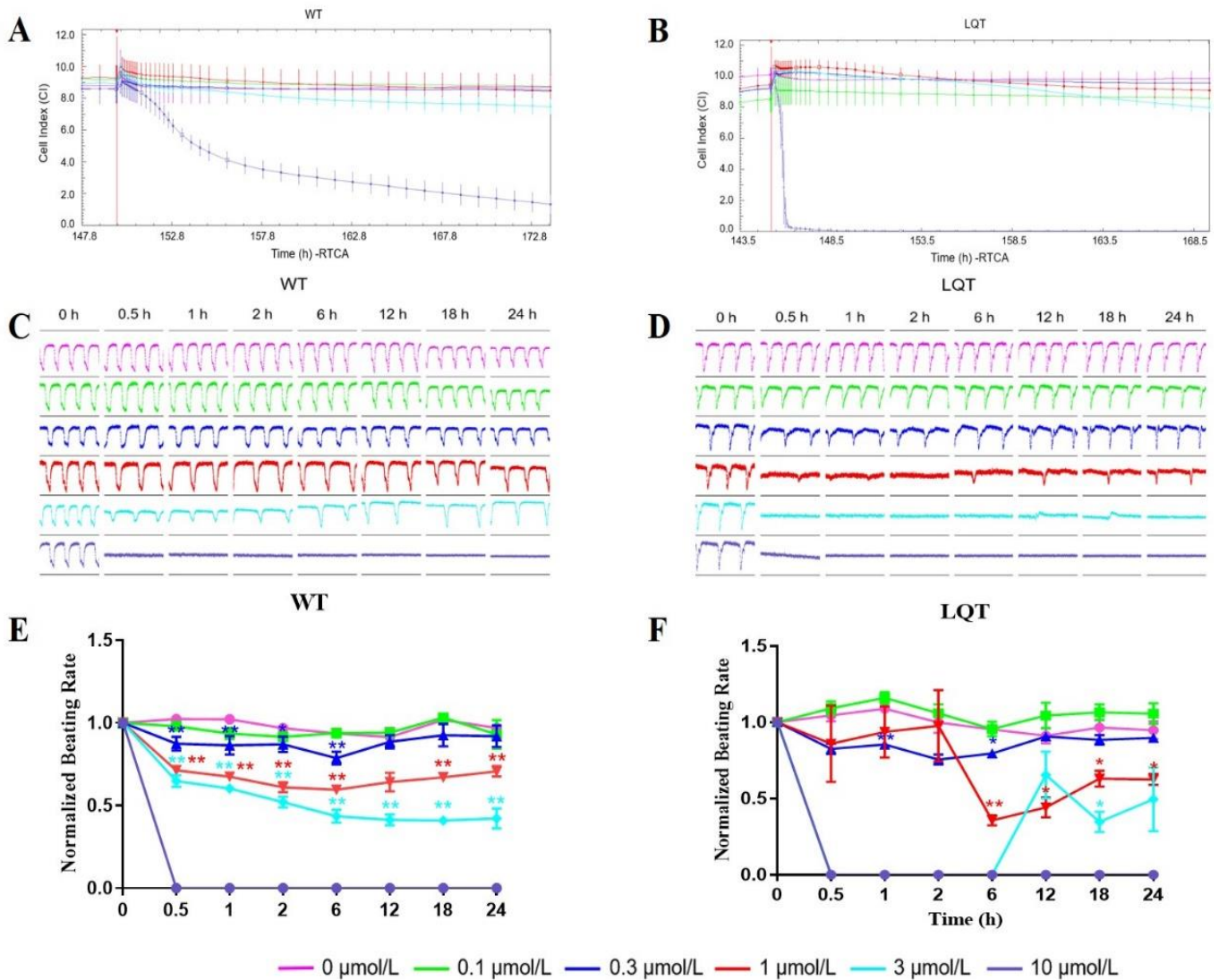


Figure 3: Effects of Sunitinib on WT- and LQT-hiPSC-CMs. Effect of Sunitinib on cell index (CI) of A WT- and B LQT-hiPSC-CMs. Effect of Sunitinib on transient pulse patterns of C WT- and D LQT-hiPSC-CMs. Effect of Sunitinib on beating rate of E WT- and F LQT-hiPSC-CMs. Data are means ± standard error of the mean (SEM) of n = 3-6 experiments. *p < 0.05 and **p < 0.01 compared to control (DMSO).

manner at concentrations $\geq 0.3 \mu\text{mol/L}$ (Figure 5E) The beating rate of LQT-hiPSC-CMs reduced in a concentration-dependent manner at concentrations $\geq 10 \mu\text{mol/L}$ while the beating rate of LQT-hiPSC-CMs increased at $0.3 \mu\text{mol/L}$ and $3 \mu\text{mol/L}$ (Figure 5F). Evaluation of the concentration-dependent effects of Dasatinib on WT- and LQT-hiPSC-CMs demonstrated IC_{50} values of $27.34 \mu\text{mol/L}$ and $23.30 \mu\text{mol/L}$, respectively (Table 2).

When both types of cell colonies were examined by fluorescence microscopy, increased CX-43 expression around some cell nuclear and decreased CX-43 expression between cell gaps was noted at $30 \mu\text{mol/L}$ on Dasatinib-treated WT- and LQT-hiPSC-CMs colonies (Figure 6A and 6B).

Dasatinib could increase the activity of Caspase-3/7 protein in a concentration-dependent manner at $\geq 0.3 \mu\text{mol/L}$ on WT (except $3 \mu\text{mol/L}$)- and LQT-hiPSC-CMs (Figure 6C).

Effects of Lapatinib: Lapatinib reduced the CI of both WT- and LQT-hiPSC-CMs in a concentration-dependent manner, indicating its inhibitory effect on the growth and adherence of cells at concentrations $\geq 10 \mu\text{mol/L}$ (Figure 7A and 7B). Lapatinib affected pulse signals of both WT- and LQT-hiPSC-CMs in a concentration-dependent manner and abolished the cellular automaticity at $3 \mu\text{mol/L}$ and $10 \mu\text{mol/L}$, but the latter CMs showed signs of recovery at $3 \mu\text{mol/L}$ (Figure 7C and 7D). The beating rate was reduced in a concentration-dependent manner at concentrations \geq

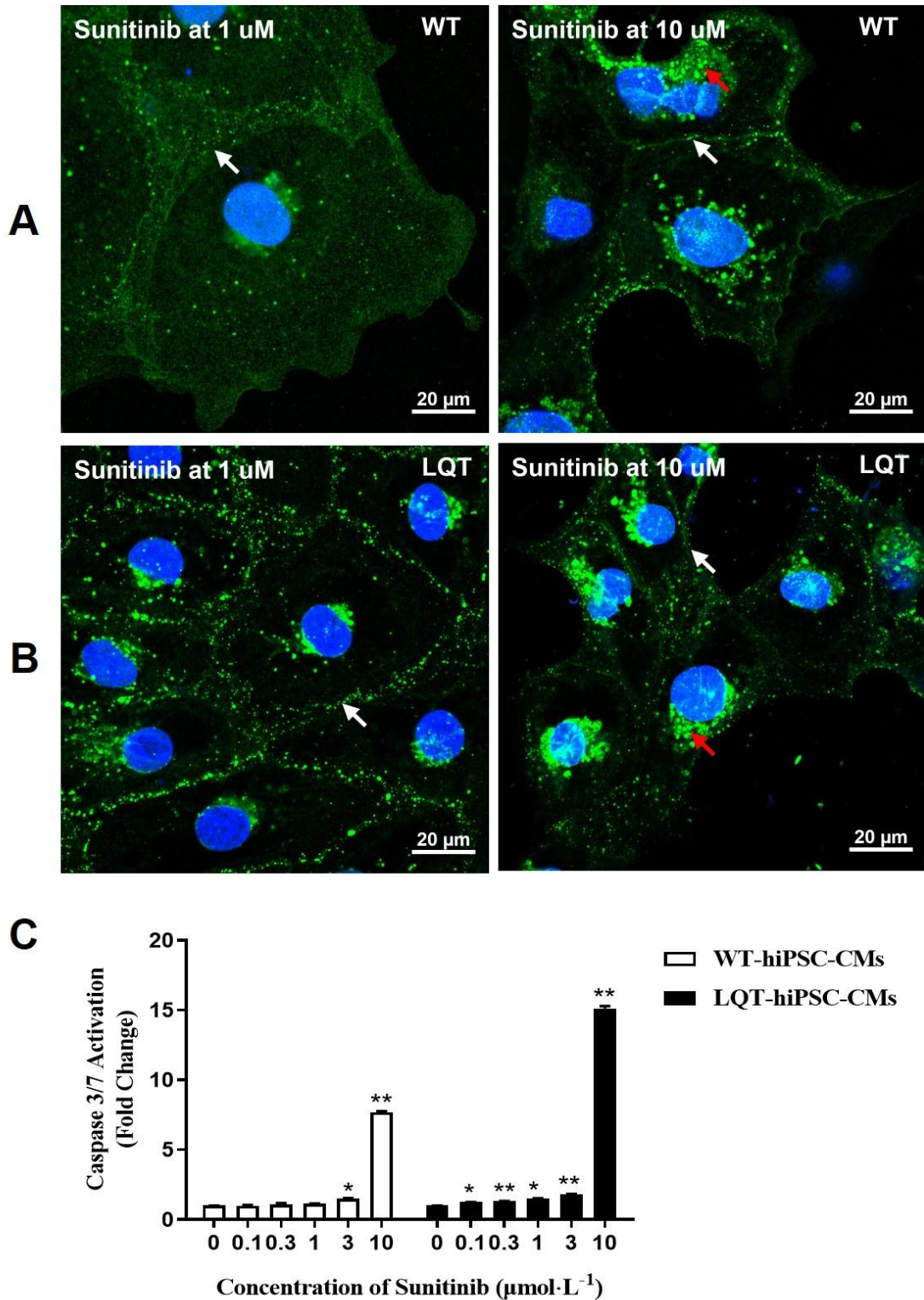


Figure 4: Effect of Sunitinib on CX-43 expression of A WT- and B LQT-hiPSC-CMs. C Effect of Sunitinib on Caspase-3/7 activation in WT- and LQT-hiPSC-CMs. Data are means \pm standard error of the mean (SEM), $n = 3$. * $p \leq 0.05$ and ** $p \leq 0.01$ compared to control (DMSO).

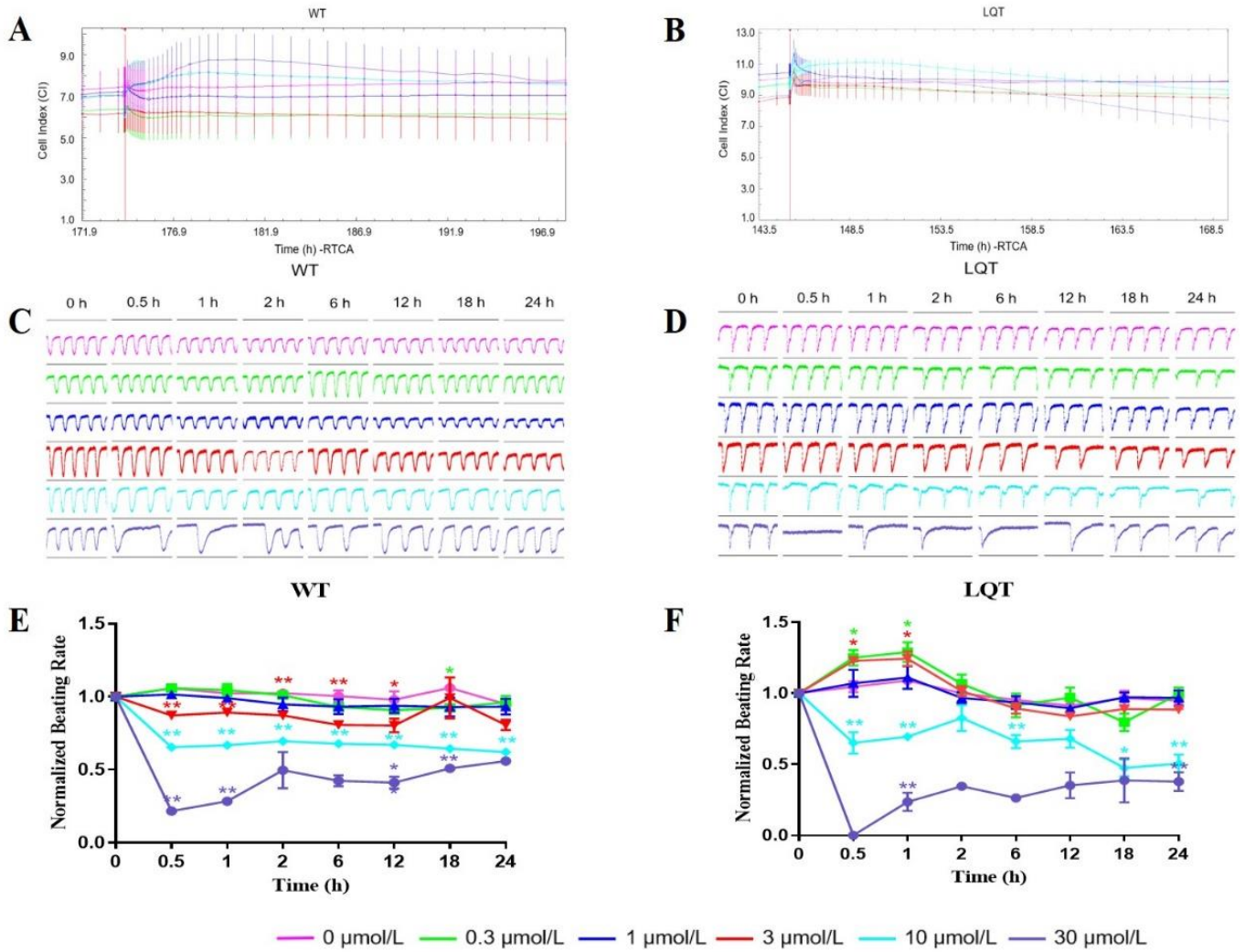


Figure 5: Effects of Dasatinib on WT- and LQT-hiPSC-CMs. Effect of Dasatinib on cell index (CI) of A WT- and B LQT-hiPSC-CMs. Effect of Dasatinib on transient pulse patterns of C WT- and D LQT-hiPSC-CMs. Effect of Dasatinib on beating rate of E WT- and F LQT-hiPSC-CMs. Data are means \pm standard error of the mean (SEM) of $n = 3-6$ experiments. * $p < 0.05$ and ** $p < 0.01$ compared to control (DMSO).

3 $\mu\text{mol/L}$ on WT-hiPSC-CMs and at concentrations ≥ 10 $\mu\text{mol/L}$ on LQT-hiPSC-CMs (Figure 7E and 7F). Evaluation of the concentration-dependent effects of Lapatinib on WT- and LQT-hiPSC-CMs demonstrated IC_{50} values of 6.87 $\mu\text{mol/L}$ and 10.89 $\mu\text{mol/L}$, respectively (Table 2).

When both types of cell colonies were examined by fluorescence microscopy, increased CX-43 expression around some cell nuclear and decreased CX-43 expression between cell gaps was noted at ≥ 3 $\mu\text{mol/L}$ and wrinkled morphology was noted at 30 $\mu\text{mol/L}$ on Lapatinib-treated WT-hiPSC-CMs colonies (Figure 8A). Decreased CX-43 expression between cell gaps was noted in a concentration-dependent manner at ≥ 3 $\mu\text{mol/L}$ on Lapatinib-treated LQT-hiPSC-CMs (Figure 8B). Lapatinib could increase the activity of Caspase-3/7

protein in a concentration-dependent manner at ≥ 10 $\mu\text{mol/L}$ on WT-hiPSC-CMs and at ≥ 30 $\mu\text{mol/L}$ on LQT-hiPSC-CMs (Figure 8C).

Discussions

Drug-induced cardiotoxicity is one of the main reasons for drug clinical trial failure or withdrawal from the market. Cardiotoxicity has received extensive attention from drug regulatory authorities and R&D institutions in various countries [8, 9]. Tyrosine kinase inhibitors, as small-molecule targeted therapy drugs, play an important role in the treatment of hematological malignancies and solid tumors, but potential cardiotoxicity and other side effects limit their efficacy [10]. Crizotinib, a receptor TKI with several targets including

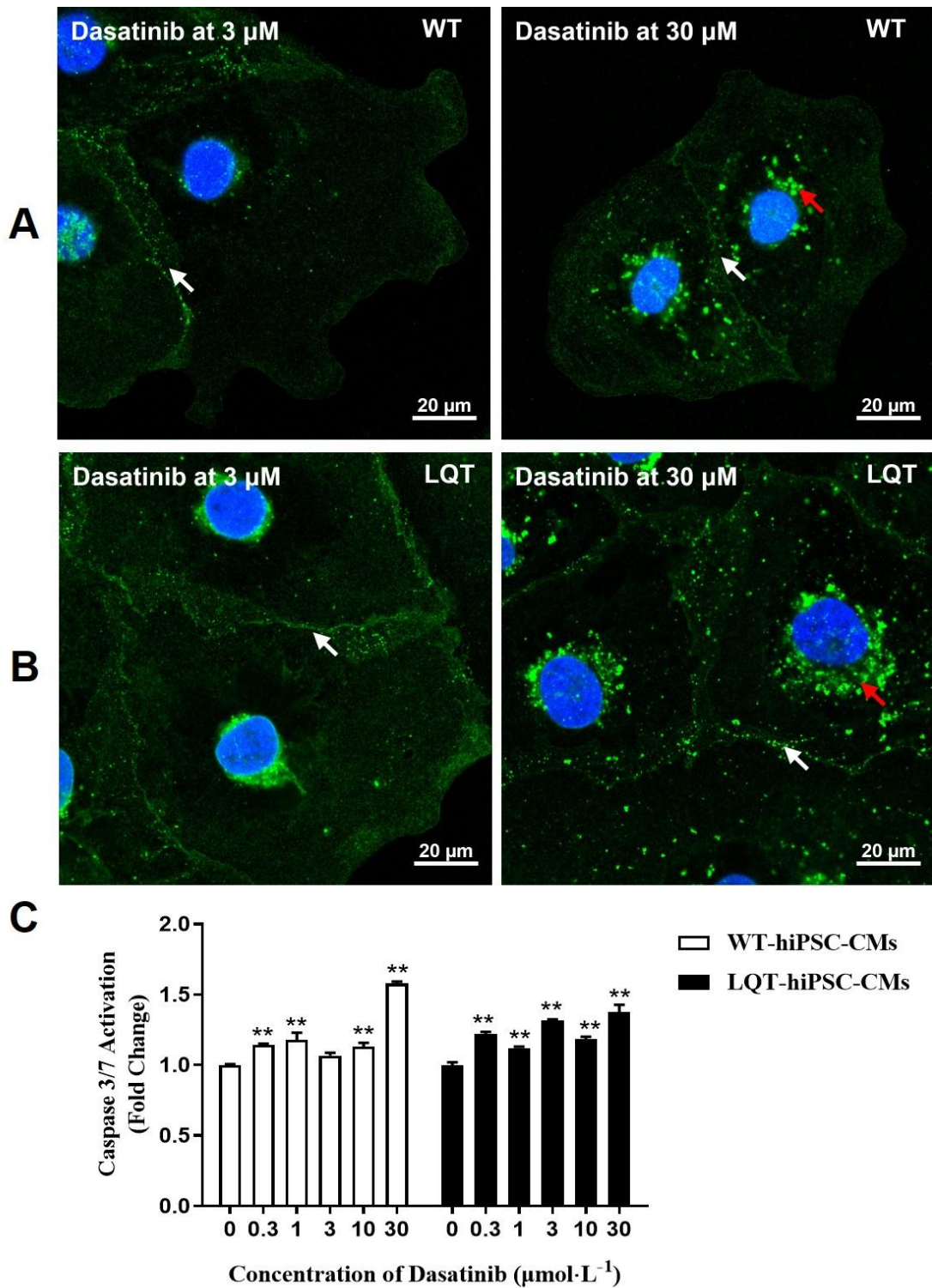


Figure 6: Effect of Dasatinib on CX-43 expression of A WT- and B LQT-hiPSC-CMs. C Effect of Dasatinib on Caspase-3/7 activation in WT- and LQT-hiPSC-CMs. Data are means ± standard error of the mean (SEM), n = 3. *p ≤ 0.05 and **p ≤ 0.01 compared to control (DMSO).

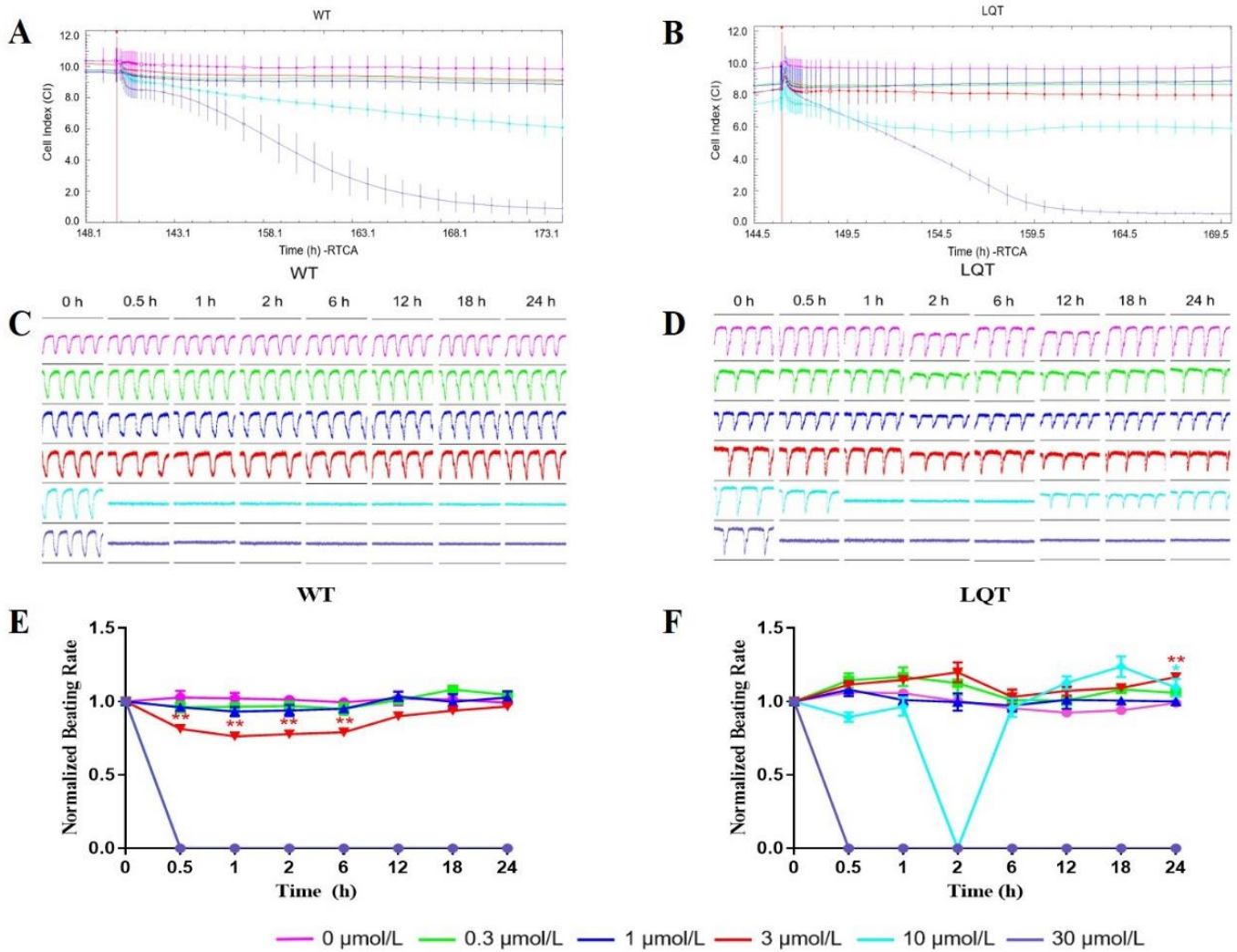


Figure 7: Effects of Lapatinib on WT- and LQT-hiPSC-CMs. Effect of Lapatinib on cell index (CI) of A WT- and B LQT-hiPSC-CMs. Effect of Lapatinib on transient pulse patterns of C WT- and D LaQT-hiPSC-CMs. Effect of Lapatinib on beating rate of E WT- and F LQT-hiPSC-CMs. Data are means \pm standard error of the mean (SEM) of $n = 3-6$ experiments. * $p < 0.05$ and ** $p < 0.01$ compared to control (DMSO).

c-ros oncogene1 (ROS1) and MET protooncogene (MET), is mainly used to treat anaplastic lymphoma kinase (ALK)-positive advanced non-small cell lung cancer (NSCLC). The most frequent Crizotinib-related cardiotoxicities reported in clinical trials were QT interval prolongation and bradycardia [11, 12]. Consistent with these clinical findings, slowing of the beating rate was observed in our study. Crizotinib reduced the CI of both WT- and LQT-hiPSC-CMs $\geq 3 \mu\text{mol/L}$ in a concentration-dependent manner, which indicates the cytotoxic effect may be the reason for the cardiotoxicity of Crizotinib. Decreased CX-43 expression between cell gaps at $\geq 1 \mu\text{mol/L}$ and increased activity of Caspase-3/7 protein at $\geq 3 \mu\text{mol/L}$ were noted on WT-hiPSC-CMs; decreased CX-43 expression between cell gaps and increased activity of Caspase-3/7 protein were noted at $\geq 1 \mu\text{mol/L}$ on LQT-

hiPSC-CMs. These findings suggested that damage to the CX-43 protein and activation of the Caspase-3/7 pathway are responsible for the negative inotropy of Crizotinib. Furthermore, LQT-hiPSC-CMs showed a higher sensitivity to Crizotinib-induced cardiotoxicity than WT-hiPSC-CMs. Sunitinib targets vascular epidermal growth factor receptor 1 (VEGFR1)-3, platelet-derived growth factor receptor (PDGFR)- α and - β , and colony-stimulating factor 1 receptor (CSF1R) [23]. This agent is known for its therapeutic effect on renal cell carcinoma, chronic myeloid leukemia, imatinib-resistant gastrointestinal stromal tumors, pancreatic cancer, and neuroendocrine tumors [2, 14, 15]. The cardiotoxicity of Sunitinib has been reported in several clinical trials and it causes hypertension and myocardial ischemia frequently because it inhibits blood circulation [16, 17]. In the

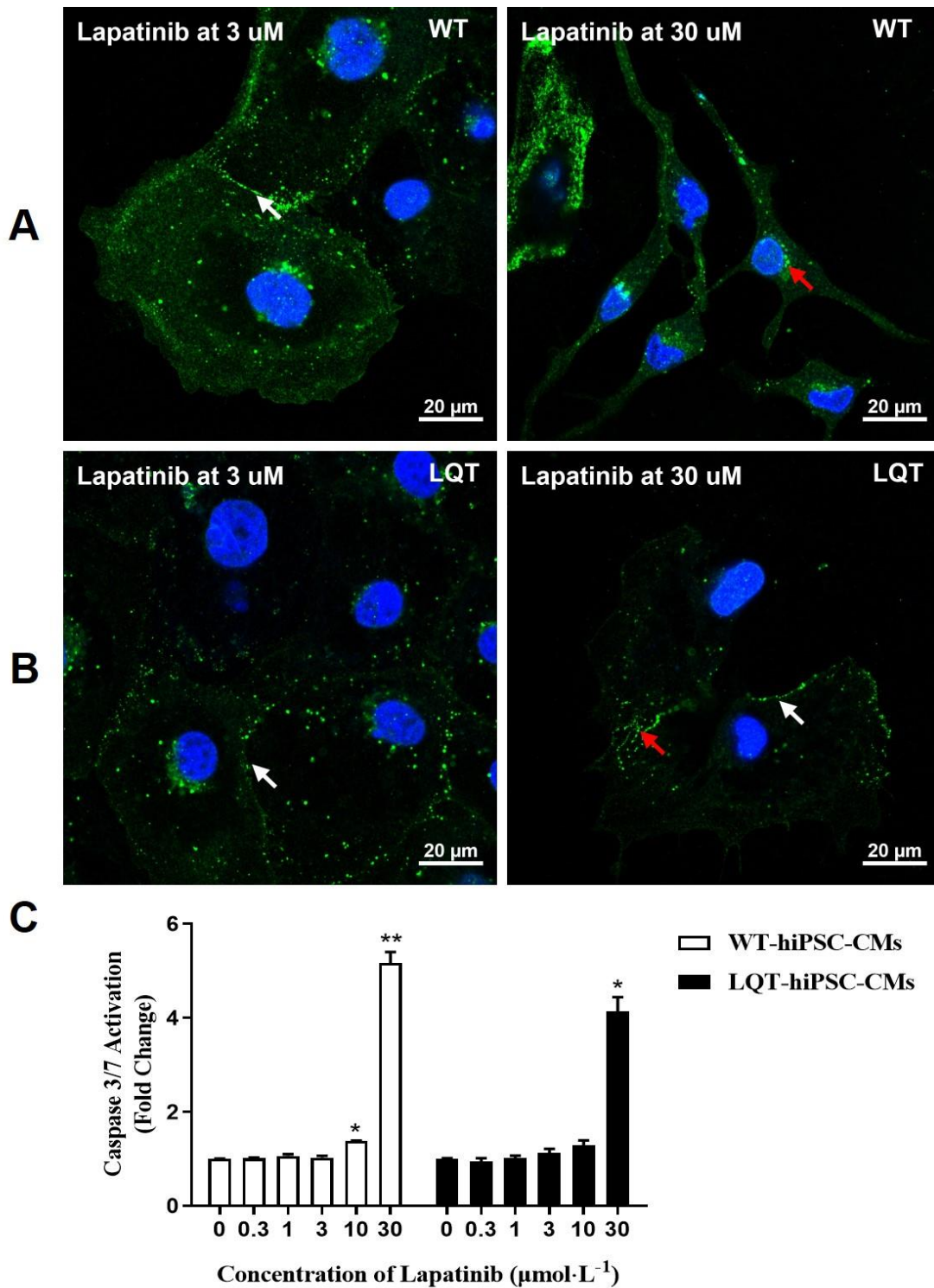


Figure 8: Effect of Lapatinib on CX-43 expression of A WT- and B LQT-hiPSC-CMs. C Effect of Lapatinib on Caspase-3/7 activation in WT- and LQT-hiPSC-CMs. Data are means \pm standard error of the mean (SEM), $n = 3$. * $p \leq 0.05$ and ** $p \leq 0.01$ compared to control (DMSO).

cardiovascular system, the tyrosine kinase inhibition induced by Sunitinib impairs cellular signal transduction, cell cycle regulation and metabolism, and transcription [18]. In our study, decreased beating rate at $\geq 0.3 \mu\text{mol/L}$ and decreased CI at $10 \mu\text{mol/L}$ were noted on WT- and LQT-hiPSC-CMs with the IC_{50} value of WT-hiPSC-CMs greater than that of LQT-hiPSC-CMs. Decreased CX-43 expression between cell gaps was noted at $\geq 1 \mu\text{mol/L}$ WT- and LQT-hiPSC-CMs. Increased activity of Caspase-3/7 protein was noted at $\geq 3 \mu\text{mol/L}$ on WT-hiPSC-CMs and at $\geq 0.1 \mu\text{mol/L}$ on LQT-hiPSC-CMs. These findings suggested that damage to the CX-43 protein and activation of the Caspase-3/7 pathway are responsible for cell apoptosis of Sunitinib. Furthermore, LQT-hiPSC-CMs showed a higher sensitivity to Sunitinib-induced cardiotoxicity than WT-hiPSC-CMs.

Dasatinib was approved by the US Food and Drug Administration (FDA) in 2006 as a small-molecule BCR-ABL1-targeted TKI. Its cardiovascular toxicities include pleural effusions, pulmonary arterial hypertension, and QT interval prolongation [19-21]. Compared to other TKIs, Dasatinib is thought to have relatively few cardiac side effects because the mean QT interval change is only 3-13 ms [22] at the therapeutic concentration combined with the C_{max} of Dasatinib at the human clinical therapeutic concentration (about $0.21 \mu\text{mol/L}$) [23]. In agreement with this notion, in this study, the effects of cardiotoxicity for Dasatinib were less than that of the other tested TKIs, although slight changes were noted in the beating rate, CX-43 expression, and the activity of Caspase-3/7 protein on both types of cells up to $30 \mu\text{mol/L}$. Lapatinib targets human epidermal growth factor receptor 2 (HER2, HER2/neu, or ErbB2) and epidermal growth factor receptor (EGFR)/HER1 and is used in combination with capecitabine for the treatment of ErbB2 overexpression in advanced or metastatic breast cancers [24]. The most common clinical manifestation of the cardiotoxicity of Lapatinib is decreased left ventricular ejection fraction (LVEF), although the underlying mechanism is still not completely understood [25]. Likewise, in our study, a decreased beating rate was noted at $\geq 3 \mu\text{mol/L}$ on WT-hiPSC-CMs and at $\geq 10 \mu\text{mol/L}$ on LQT-hiPSC-CMs. Additionally, decreased CI at $\geq 10 \mu\text{mol/L}$ and decreased CX-43 expression between cell gaps at $\geq 3 \mu\text{mol/L}$ were noted on both WT- and LQT-hiPSC-CMs, and an increase the activity of Caspase-3/7 protein was noted at $\geq 10 \mu\text{mol/L}$ on WT-hiPSC-CMs and at $\geq 30 \mu\text{mol/L}$ on LQT-hiPSC-CMs. However, the effects of Lapatinib on the beating rate and the activity of Caspase-3/7 protein of both WT- and LQT-hiPSC-CMs were basically the same by comparing the IC_{50} values of Lapatinib on the beating rate and the Caspase-3/7 protein content of the two type's cells.

Conclusions

In conclusion, we found that WT-hiPSC-CMs and LQT-hiPSC-CMs from different sources exhibited similar

responses to several TKIs. When reached a relatively stable state, the two types of cells' beat frequency, amplitude, and irregularity index were basically the same. Of the four tested drugs, Crizotinib, Sunitinib, and Lapatinib induced a higher degree of cardiotoxicity than Dasatinib, and Dasatinib was considered to be a relatively safe and effective drug, as previously reported. The current study provides valuable information on the mechanisms by which TKIs affect cardiac myocardial contraction of both WT- and LQT-hiPSC-CMs. Moreover, LQT-hiPSC-CMs showed a higher sensitivity to Crizotinib and Sunitinib-induced cardiotoxicity than WT-hiPSC-CMs, which indicates LQT1 patients should exercise extreme caution with Crizotinib and Sunitinib. The results of this study could contribute to providing a platform for precision medicine and drug screening in the future. HiPSC-CMs from healthy volunteers have the potential used for drug screening and cardiotoxicity evaluation, providing a more complete understanding of the mechanism of drug cardiotoxicity. HiPSC-CMs from patients could be used to understand disease mechanisms and screened therapeutic drugs, which is conducive to the development of personalized diagnosis and treatment.

Authors contributions

#QZ and #YZ contributed equally. XW and QZ designed the research. YZ and HX performed the experiments. YZ, YT, and HY prepared all figures. QZ and YZ wrote the main manuscript text. XW and QZ revised the manuscript text and figures and provided scientific suggestions. All authors analyzed the data, reviewed the manuscript, and read and approved the final manuscript.

Acknowledgment

We thank Cellapy and HELP for providing stable hiPSC-CMs.

Funding

This study was supported by the Shanghai Foundation of Science and Technology (21DZ2291000).

Conflict of interest statement

The authors declare that they have no competing interests.

Abbreviations

TKI, tyrosine kinase inhibitor; WT, wild type; hiPSC-CMs, human induced pluripotent stem cell-derived cardiomyocytes; IC_{50} , half maximal inhibitory concentration; LQT, long QT syndrome; RTCA, xCELLigence® real-time cell analysis; CI, cell index; APD, action potential duration; AP, action potential; DMSO, dimethyl sulfoxide; ALK, anaplastic lymphoma kinase; EGFR, epidermal growth factor receptor; CSF1R, colony-stimulating factor 1 receptor; FDA, US Food and Drug Administration; HER2, human epidermal

growth factor receptor 2; LVEF, left ventricular ejection fraction; MET, MET protooncogene; NSCLC, non-small cell lung cancer; PDGFR, platelet-derived growth factor receptor; ROS, reactive oxygen species; ROS1, c-ros oncogene1; KCNQ1, Potassium voltage-gated channel subfamily Q member 1.

References

- Zarifa A, Albittar A, Kim P Y, et al. Cardiac toxicities of anticancer treatments: chemotherapy, targeted therapy and immunotherapy[J]. *Current opinion in cardiology* 34 (2019): 441-450.
- Mellor HR, Bell AR, Valentin JP, et al. Cardiotoxicity associated with targeting kinase pathways in cancer. *Toxicol Sci* 120 (2011): 14-32.
- Pourrier M, Fedida D. The Emergence of Human Induced Pluripotent Stem Cell-Derived Cardiomyocytes (hiPSC-CMs) as a Platform to Model Arrhythmic Diseases. *Int J Mol Sci* 21 (2020): E657.
- Magdy T, Schuldt A J T, Wu J C, et al. Human Induced Pluripotent Stem Cell (hiPSC)-Derived Cells to Assess Drug Cardiotoxicity: Opportunities and Problems[J]. *Annu Rev Pharmacol Toxicol* 58 (2018): 83-103.
- Yoshida Y, Yamanaka S. Induced Pluripotent Stem Cells 10 Years Later: For Cardiac Applications [J]. *Circ Res* 120 (2017): 1958-1968.
- Moretti A, Bellin M, Welling A, et al. Patient-specific induced pluripotent stem-cell models for long-QT syndrome [J]. *N Engl J Med* 363 (2010): 1397-1409.
- Zhao Q, Wang X, Wang S, et al. Cardiotoxicity evaluation using human embryonic stem cells and induced pluripotent stem cell-derived cardiomyocytes [J]. *Stem cell research & therapy* 8(2017): 1-7.
- Varga Z V, Ferdinandy P, Liaudet L, et al. Drug-induced mitochondrial dysfunction and cardiotoxicity [J]. *Am J Physiol Heart Circ Physiol* 309 (2015): H1453-1467.
- Onakpoya I J, Heneghan C J, Aronson J K. Post-marketing regulation of medicines withdrawn from the market because of drug-attributed deaths: an analysis of justification [J]. *Drug safety* 40 (2017): 431-441.
- Srikanthan A, Ethier J L, Ocana A, et al. Cardiovascular toxicity of multi-tyrosine kinase inhibitors in advanced solid tumors: a population-based observational study [J]. *PLoS One* 10 (2015): e0122735.
- Shaw A T, Ou S H I, Bang Y J, et al. Crizotinib in ROS1-rearranged non-small-cell lung cancer[J]. *New England Journal of Medicine* 371 (2014): 1963-1971.
- Tartarone A, Gallucci G, Lazzari C, et al. Crizotinib-induced cardiotoxicity: the importance of a proactive monitoring and management[J]. *Future Oncology* 11 (2015): 2043-2048.
- Gallucci G, Tartarone A, Lombardi L, et al. When Crizotinib-induced bradycardia becomes symptomatic: role of concomitant drugs[J]. *Expert Review of Anticancer Therapy* 15 (2015): 761-763.
- Yun H J, Seo Y J, Lee H J. Gray hair associated with the multitargeted receptor tyrosine kinase inhibitor pazopanib[J]. *Annals of Dermatology* 27 (2015): 791-792.
- Richards C J, Je Y, Schutz F A, et al. Incidence and risk of congestive heart failure in patients with renal and nonrenal cell carcinoma treated with Sunitinib [J]. *J Clin Oncol* 29 (2011): 3450-3456.
- Dobbin S J H, Cameron A C, Petrie M C, et al. Toxicity of cancer therapy: what the cardiologist needs to know about angiogenesis inhibitors [J]. *Heart* 104 (2018): 1995-2002.
- Chaar M, Kamta J, Ait-Oudhia S. Mechanisms, monitoring, and management of tyrosine kinase inhibitors-associated cardiovascular toxicities [J]. *OncoTargets and therapy* 11 (2018): 6227.
- Yang Y, Bu P. Progress on the cardiotoxicity of Sunitinib: Prognostic significance, mechanism and protective therapies [J]. *Chemico-Biological Interactions* 257 (2016): 125-131.
- Caldemeyer L, Dugan M, Edwards J, et al. Long-term side effects of tyrosine kinase inhibitors in chronic myeloid leukemia [J]. *Current hematologic malignancy reports* 11 (2016): 71-79.
- Keating G M. Dasatinib: a review in chronic myeloid leukaemia and Ph+ acute lymphoblastic leukaemia [J]. *Drugs* 77 (2017): 85-96.
- Chaar M, Kamta J, Ait-Oudhia S. Mechanisms, monitoring, and management of tyrosine kinase inhibitors-associated cardiovascular toxicities [J]. *OncoTargets and therapy* 11 (2018): 6227.
- Damrongwatanasuk R, Fradley M G. Cardiovascular complications of targeted therapies for chronic myeloid leukemia[J]. *Current treatment options in cardiovascular medicine* 19 (2017): 1-13.
- Izumi-Nakaseko H, Fujiyoshi M, Hagiwara-Nagasawa M, et al. Dasatinib can impair left ventricular mechanical function but may lack proarrhythmic effect: A proposal of non-clinical guidance for predicting clinical cardiovascular adverse events of tyrosine kinase inhibitors [J]. *Cardiovascular Toxicology* 20 (2020): 58-70.

24. Choi H D, Chang M J. Cardiac toxicities of Lapatinib in patients with breast cancer and other HER2-positive cancers: a meta-analysis [J]. Breast cancer research and treatment 166 (2017): 927-936.
25. Jerusalem G, Lancellotti P, Kim S B. HER2+ breast cancer treatment and cardiotoxicity: monitoring and management [J]. Breast cancer research and treatment 177 (2019): 237-250.

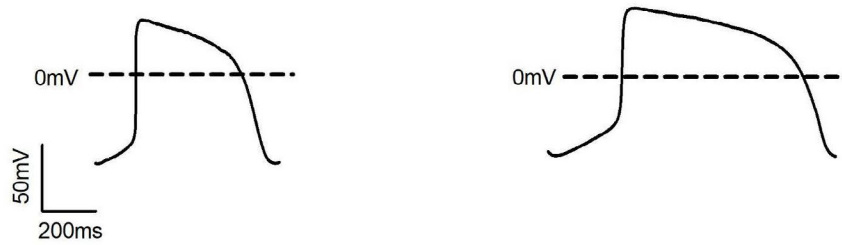


Patch clamp analysis of NovoCell™ Cardiomyocytes

Electrophysiological characteristics of NovoCell™ Cardiomyocytes were analyzed by manual patch clamp.

Electrophysiological characteristics

Test parameter	Action Potential	RMP (mV)	APA (mV)	APD90 (ms)	APD50 (ms)	Vmax (V/S)
Result	Ventricular-like	-63 ± 3	108 ± 1	502 ± 89	450 ± 80	34 ± 17



Representative ventricular-like action potential profiles of NovoCell™ Cardiomyocytes from the same batch.

艾尔普再生医学科技有限公司
Help Stem Cell Innovations Co., Ltd.

www.helpsci.com.cn



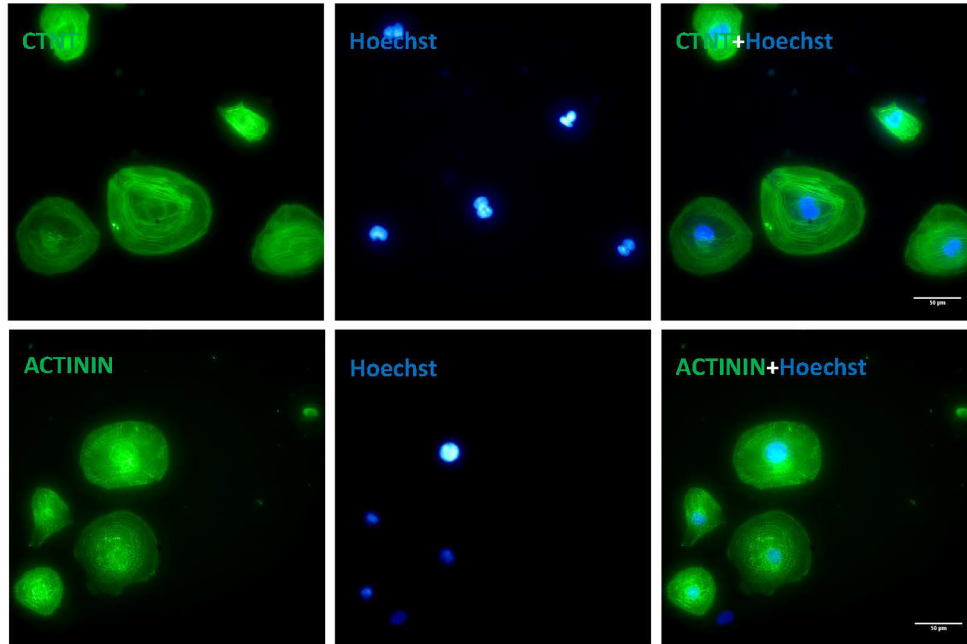
025-6602 0502

wangjx@helpsci.com.cn

江苏省南京市江宁区龙眠大道568
生命科技创新园1号楼4A



Immunofluorescence analysis of α -Actinin and cTnT expression in NovoCell™ Cardiomyocytes
NovoCell™ Cardiomyocytes were labeled for α -actinin and cTnT (Green). Nuclei were labeled with Hoechst (Blue).



Bar=50 μ m

艾尔普再生医学科技有限公司
Help Stem Cell Innovations Co., Ltd.

www.helpsci.com.cn



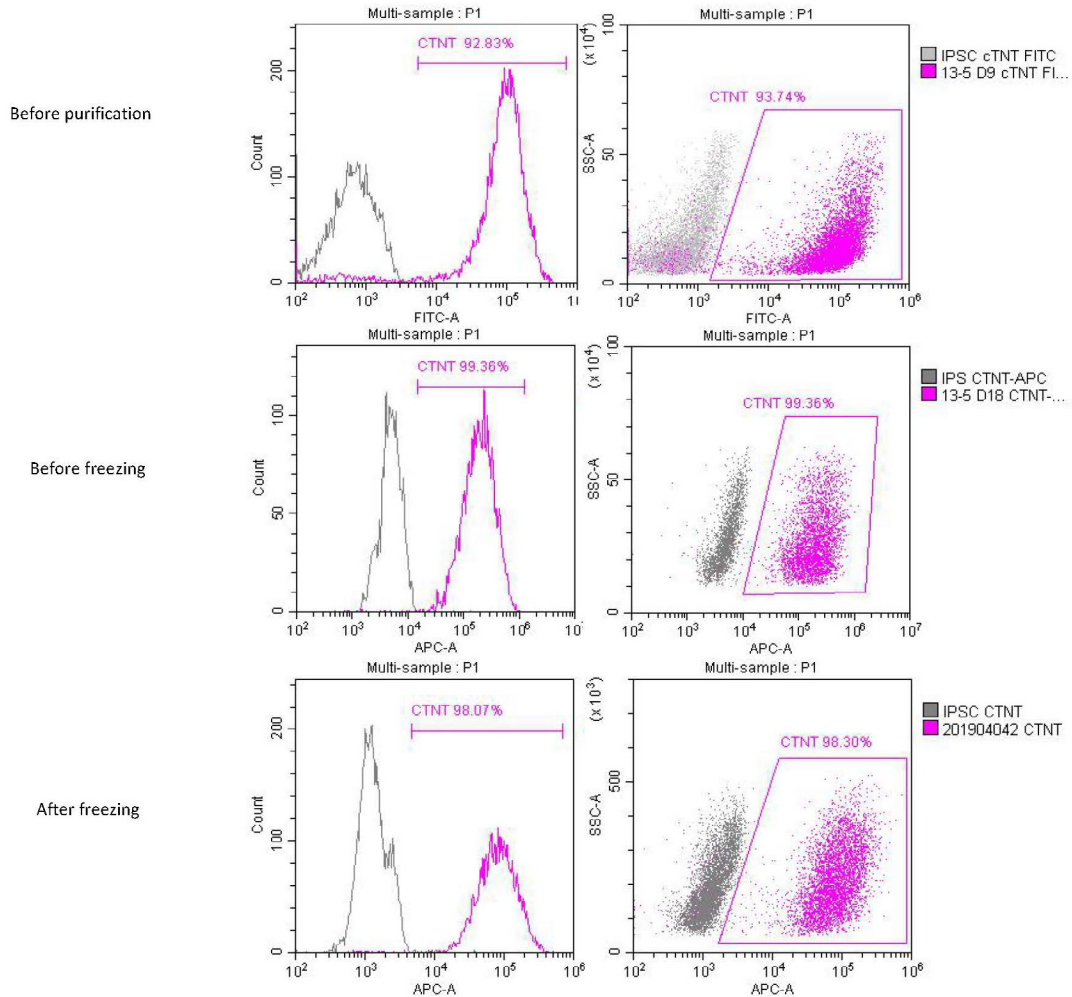
025-6602 0502

wangjx@helpsci.com.cn

江苏省南京市江宁区龙眠大道568
生命科技创新园1号楼4A



Flow cytometry analysis of cardiomyocyte marker cTnT expression in NovoCell™ Cardiomyocytes
NovoCell™ Cardiomyocytes were labeled for cTnT to ensure purity.



艾尔普再生医学科技有限公司
Help Stem Cell Innovations Co., Ltd.

www.helpsci.com.cn



025-6602 0502
wangjx@helpsci.com.cn
江苏省南京市江宁区龙眠大道568
生命科技创新园1号楼4A



CERTIFICATE OF ANALYSIS

PRODUCT: NovoCell™ Cardiomyocytes
 CAT NO.: NC20300002
 LOT NO.: 201904042
 DATE OF REPORT: 20 May 2019

PRODUCT DESCRIPTION

NovoCell™ Cardiomyocytes are human iPSC-derived cardiomyocytes suitable for drug screening, toxicity evaluation and other *in vitro* applications.
 This product was manufactured in a GMP facility.

Viability

TEST DESCRIPTION	SPECIFICATION	RESULT
Cell Number	$\geq 2 \times 10^6$ cells	Pass
Post-Thaw Recovery	>70% adhere	Pass

Sterility

TEST DESCRIPTION	SPECIFICATION	RESULT
Bacteria	Negative	Pass
Fungi (Yeast and Mold)	Negative	Pass
Mycoplasma	Negative	Pass

Characterization

PLURIPOTENCY MARKERS	SPECIFICATION	RESULT
Cardiac Troponin T (cTnT)	>90% cTnT	Pass

艾尔普再生医学科技有限公司
 Help Stem Cell Innovations Co., Ltd.

www.helpsci.com.cn



025-6602 0502
 wangjx@helpsci.com.cn
 江苏省南京市江宁区龙眠大道568
 生命科技创新园1号楼4A

CERTIFICATE OF ANALYSIS

PRODUCT: CardioEasy® Human Cardiomyocytes

Cat NO.: CA2201106

LOT NO.: FH18GI162

PRODUCT DESCRIPTION

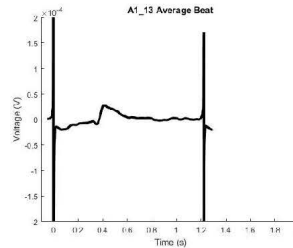
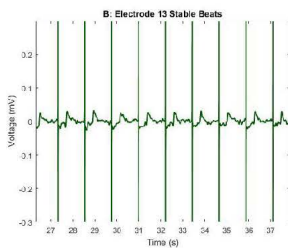
CardioEasy® Human Cardiomyocytes are a ready-to-use, high purity human iPSC-derived cardiomyocytes suitable for drug screening, toxicity evaluation and other in vitro applications. The product is produced using the highly efficient cardiomyocytes directed differentiation and purification of Cellapy® Co.,LTD..

TEST PARAMETER:

Test Description	Specification	Result
Viable Cells/Vial	1.0×10 ⁶ at thaw by trypan blue exclusion	Pass
Mycoplasma	No contamination detected	Pass
Sterility	No contamination detected	Pass

MICROELECTRODE ARRAY TEST:

Test Parameter:	Beat Period(s)	FPD(ms)	FPDc(Fridericia ms)	Spike Amplitude (mV)
Result	1.3 ± 0.1	412 ± 33	381 ± 32	0.6 ± 0.3



DATE: 3 August 2018